Cavity ring down spectroscopy on radicals in a supersonic slit nozzle discharge

Tomasz Motylewski and Harold Linnartz
Institute for Physical Chemistry, University of Basel, Klingelbergstrasse 80, CH 4056 Basel, Switzerland

(Received 9 September 1998; accepted for publication 26 October 1998)

A sensitive and generally applicable technique for direct absorption spectroscopy on electronic transitions of transient species in the gas phase is presented. The method is based on cavity ring down spectroscopy in a pulsed slit nozzle, incorporating a discharge in a high pressure supersonic expansion. The performance is demonstrated with spectra of the 0_0^0 origin band of the $^2\Pi \leftarrow X^2\Pi$ electronic transition of the isoelectronic linear carbon chain radicals C_6H and $C_6H_2^+$. Rotationally resolved and rotationally cold spectra ($T_{rot} < 15$ K) have been obtained. The sensitivity of the technique is demonstrated for anions with a detection limit as low as 10^7 C_2^- molecules cm^{-3} for rovibrational transitions of the $B^2\Sigma_u^+ \leftarrow X^2\Sigma_g^+$ system. © *1999 American Institute of Physics.* [S0034-6748(99)01002-3]

I. INTRODUCTION

Transient molecules, as radicals and ions, belong to the chemically most reactive species. They play a key role in many processes, varying from atmospheric and interstellar to combustion and biochemistry. This high reactivity, however, also complicates systematic spectroscopic studies, as it is hard to generate large abundances under laboratory controlled conditions. In the past several methods have been developed to circumvent this problem. The initial direct absorption experiments in the microwave and infrared mainly used electrical discharges in long and cryogenically cooled cells.[1–3] Uniform plasmas with high molecular densities were obtained in hollow cathode geometries[4] or magnetically enhanced negative glow discharges.[5] In both cases, the larger part of the discharge consists of a negative glow. Velocity modulation in the positive column of a normal discharge further increased the detection limit of molecular ions and it simultaneously offered an experimental way for distinguishing the spectra of neutral and charged species.[6] Although these cell techniques form effective methods for the production of radicals and molecular ions, the spectroscopy generally suffers from high rovibrational temperatures and Doppler limited resolution. Under these conditions spectra of even simple systems can become rather congested, whereas on the other hand single spectral lines may hide fine or hyperfine splittings. The high temperatures furthermore decrease the quantum state population density, which affects the overall sensitivity of the experiment.

These disadvantages can be overcome by combining supersonic expansion and plasma techniques. The first attempt in this direction was reported in 1983[7,8] and describes a single pin discharge via a continuous gas flow through a small circular nozzle. The source was used successfully for several emission and laser-induced fluorescence studies on rotationally cold radicals,[9] but for direct absorption spectroscopic techniques the effective pathlength turned out to be too small. This necessitated the introduction of larger systems,[10] which resulted in the use of slit nozzles.[11,12] These provide a Doppler free environment and combine high molecular densities and relatively large absorption pathlengths with an effective adiabatical cooling. In addition the density in the expansion falls off linearly with the distance downstream, whereas in pinhole expansions this is quadratically. Consequently, the number of cooling collisions in slit jet expansions is larger than in any of the other geometries, which also explains that slit nozzles have been successfully used to study numerous weakly bound molecular complexes. It is a logical continuation to combine slit nozzle and plasma techniques in order to achieve absolute radical and ion densities equivalent to or higher than in long-pass cell geometries. However, this has long been hindered by the lack of a method that generates a stable plasma over the total length of the slit. In recent years four different methods have been proposed to solve the problem.

Excimer ablation of a carbon rod in the throat of the slit has been used for the high resolution infrared study of long neutral carbon chain radicals,[13] up to C_{13}.[14] In a similar way *photolysis* of precursor gases has yielded spectra of jet cooled radicals.[15,16] Most of the efforts in recent years has been put in the development of an appropriate *discharge* geometry.[17–26] Radicals as NH_2 were observed with tunable diode laser spectroscopy in a continuous discharge across sharp jaws defining the orifice.[17] A multiple electrode version of the single pin design[7] has been used to generate a continuous plasma for direct absorption spectroscopy of molecular ions in the far infrared.[18] Rotationally cold infrared spectra of H_3^+, N_2H^+, and H_3O^+ have been measured with a continuous hollow cathode design.[19] The signal-to-noise ratios for these ions were improved substantially by changing to a cw expansion excited by a single corona pin behind the slit nozzle.[21] Especially, in the past few years considerable progress has been achieved with pulsed supersonic discharge plasmas.[22,24] Several groups have reported discharge and modulation schemes, effectively compensating for the low duty cycles, allowing direct absorption spectroscopic studies of unstable species in the microwave,[25] infrared,[23] and vis-

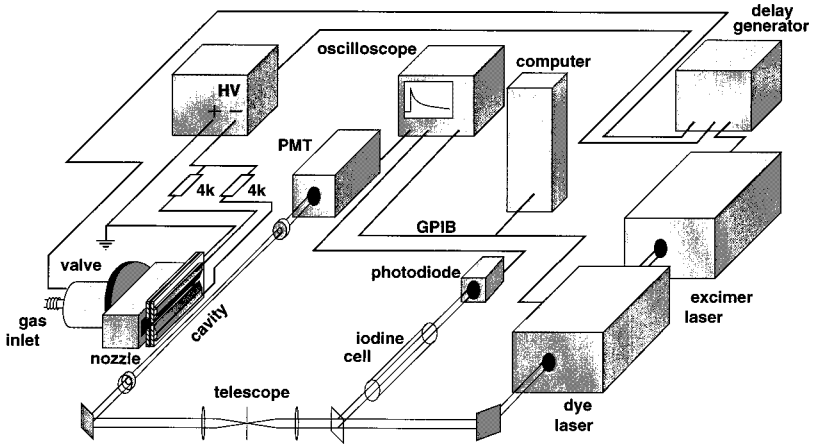

FIG. 1. Schematic diagram of the experimental setup.

ible part[26] of the electromagnetic spectrum. Finally, low energetic supersonically cooled plasmas have been obtained by combining a slit nozzle expansion with *electron impact ionization*.[27] With this technique the first direct measurement in the infrared of weakly bound ionic complexes became possible,[28,29] as well as a detailed spectroscopic characterization of the linear and centrosymmetric N_4^+ ion.[30,31]

In this experiment a pulsed slit nozzle discharge is combined with cavity ring down spectroscopy (CRDS). The source is mounted in a stable optical resonator that is formed by two highly reflective plano concave mirrors (reflectivity $>99.99\%$, $f=100$ cm). A small fraction of laser light is coupled into the cavity and the rate of light leaking out of the cavity is characterized with the ring down signal. This signal has an envelope which is simply a first order decay $\exp[-t/\tau]$. It can be easily seen that the ring down time, τ, is determined by

$$\frac{L}{c(1-R+\alpha l)},$$

where L is the optical length of the cavity, c the speed of light, R the averaged reflectivity of the two mirrors and αl the absorbance for a sample present in the cavity with absorption coefficient α and length l, i.e., the ring down time reflects the rate of absorption rather than the magnitude of the absorption and as such it has important advantages compared with conventional absorption techniques. The method is immune to pulse-to-pulse fluctuations in the laser power and the very long absorption pathlengths that are obtained by confining the light pulse several microseconds in the cavity, make this technique ideal to study unstable species.

Since its introduction[32] the technique has been applied in many different fields, varying from hostile environments as in flames and combustion,[33] samples in ultrahigh magnetic fields,[34] to discharges[35–37] and molecular beam expansions.[38–41] Both pulsed and cw lasers,[42,43] narrow band and polychromatic light sources,[44] even a free electron laser[45] have been used successfully, with applications ranging from the assignment of diffuse interstellar bands[24] to the spectroscopic characterization of biological relevant systems.[46] This shows that cavity ring down spectroscopy, especially in view of its conceptual simplicity, has become a standard technique besides established methods as resonance enhanced multiphoton ionization (REMPI) or light induced fluorescence (LIF). In two recent review articles[47,48] more applications of CRDS are discussed. Its present limitation is mainly caused by the availability of suitable highly reflective mirrors.

In this contribution a cavity ring down setup is described for the study of electronic transitions of unstable species that are generated in an adiabatically cooled slit nozzle plasma. The operation of the system is demonstrated with results on positively charged, neutral, and negatively charged carbon chain radicals.

II. EXPERIMENT

A. Cavity ring down arrangement

The experimental setup consists of a standard cavity ring down unit sampling the plasma generated in a pulsed supersonic slit jet expansion (Fig. 1). The latter is located in a large stainless-steel cross piece, evacuated by a roots blower system with a total pumping capacity of 2775 m^3/h. The mirror housings of the cavity mirrors are connected with flexible bellows to the opposite sides of the cross piece, defining a cavity of 52 cm. The alignment is achieved by adjusting high precision threaded screws. Two tilted quartz windows are fixed outside the cavity and seal the chamber. The deposition of contaminants on the super mirrors is prohibited by helium curtains and a system of small diaphragms. The distance of the orifice to the optical axis is variable during jet operation from 0 to 17 mm via a translation stage.

The tunable radiation is generated by an excimer pumped dye laser system with a maximum resolution of 0.035 cm^{-1} using an etalon in the dye laser cavity. The laser light is focused into the optical cavity and spatially filtered by means of a 1:1 telescope equipped with a 100 μm pinhole. The light exiting the ring down cavity is detected by a photomultiplier. This signal is displayed on a 300 MHz 8-bit digital oscilloscope. Typically 45 ring down events are averaged at each wavelength before the digitized data are downloaded to a workstation, that is also used to control the scanning procedure. The typical ring down time lasts from 30 to 70 μs, mainly depending on the quality of the mirrors. This corresponds to an effective absorption pathlength of approximately 1 km through a 30 mm jet. Two gates, one set at the beginning and the other at 2–3 τ of the decay curve, are used

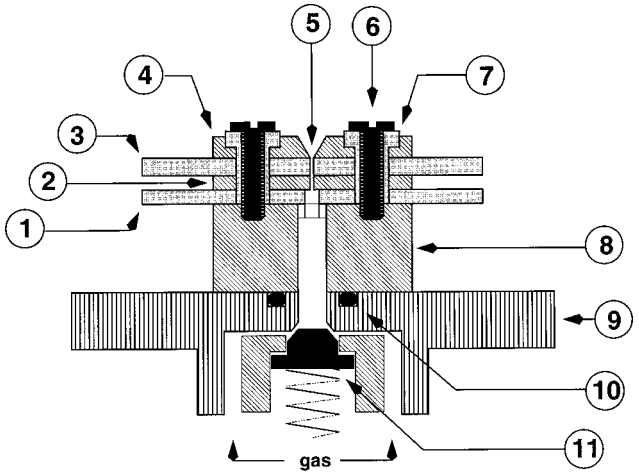

FIG. 2. Cross section of the high pressure pulsed supersonic slit nozzle discharge. The orifice consists of a ceramic insulator (1), a metal plate that is grounded (2), a second insulator (3), and two sharp stainless steel jaws (4) that form the actual slit of 30 mm×250 μm (5). Both insulators and metal parts are mounted to the body of the nozzle by electrically isolated screws (6),(7). A pulsed negative high voltage (−600 to −1200 V, 150–300 μs) is applied to the jaws via 4 kΩ ballast resistors at the moment that a high pressure pulse (10 bar) expands through the channel. The discharge strikes to the grounded plate, localizing the reaction zone to a region upstream of the expansion. The floating body of the nozzle (8) is connected to an electromagnetic driven pulsed valve (9) via an O-ring seal (10). A small plastic poppet (11) controls the gas flow into the nozzle volume. [Reprinted from H. Linnartz *et al.*, Chem. Phys. Lett. **292**, 188 (1998) with permission from Elsevier Science.]

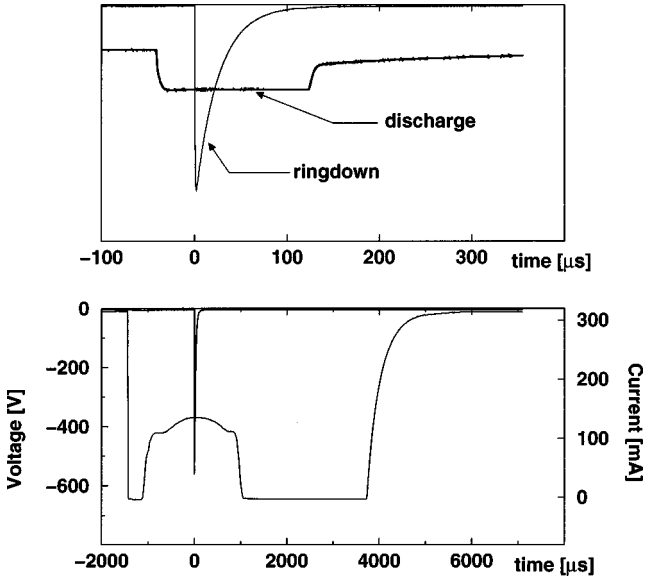

FIG. 3. The length of the discharge pulse is set to the same order as the CRD exponential decay curve, typically 150–300 μs (upper trace). The gas pulse through the slit, however, lasts much longer. This can be visualized by extending the length of the discharge pulse to several ms and by monitoring the voltage at one of the jaws (lower trace). For a pressure of 10 bar the typical length of the gas pulse through the slit amounts to approximately 1100 μs. In addition, the voltage characteristics provide direct information on the actual discharge voltage and discharge current (see vertical axes).

to determine the exponential waveform. A third time gate is used for background subtraction. A narrow band pass filter in front of the photomultiplier reduces background light from the discharge. The absolute wavelength calibration is achieved via simultaneous measurement of the absorption spectrum of molecular iodine in a room-temperature cell or a neon hollow cathode optogalvanic cell. Additional calibration and linearization programs allow a precise frequency determination.

B. Slit jet discharge

The carbon chain radicals were produced in a pulsed slit nozzle incorporating a discharge in a high pressure expansion. A detailed cross section is shown in Fig. 2. The orifice of the slit comprises an insulator, a metal plate, a second insulator, and two jaws that form the actual slit [typically 30 (or 60) mm×250 μm, 60° exit angle]. The position of the jaws is variable and slit widths of 50–300 μm can be chosen. The exact size and uniformity of the slit is defined by precision spacers that are mounted between the plates and removed after assembly. A pulsed valve (2 mm orifice) is mounted on top of the slit nozzle body and controls the gas flow into the system through a short circular channel. This channel shades off into a 1×1×30 (or 60) mm volume inside the body.

Both metal plate (1 mm thick) and insulators (1 and 1.5 mm thick) have slit openings of the same dimension as the slit orifice. In this way a two-dimensional multilayer channel is formed by the plates, that are mounted to the body by electrically isolated screws. The volume inside the body has been kept as small as possible, in order to keep the length of the final gas pulse through the slit as close as possible to the initial opening time of the pulsed valve on top of the body. A small reservoir in front of the valve operates as gas buffer zone and guarantees a stable gas flow into the slit nozzle. Typical backing pressures of ≈10 bar are used. The pressure in the vacuum setup is computer controlled and kept constant (0.1 mbar) during jet operation by adjusting the pulse length of the valve. This procedure significantly reduces fluctuations in the radical production.

A pulsed negative voltage of −600 to −1200 V is applied to both jaws via two separate 4 kΩ ballast resistors. The inner metal plate is grounded while the body floats. The latter is important in order to shield the pulsed valve from internal high voltage arcing. It furthermore prohibits carbon dust formation inside the body, which is a necessary condition for proper operation. Generally mixtures of 0.2%–0.5% C_2H_2 (or C_2D_2) in He have been used.

The geometry of the multichannel layer is such that the discharge is confined upstream of the supersonic expansion. This results in a much more efficient cooling as in multiple pin or hollow cathode like devices,[18,21] as the localized discharge before the expansion does not interfere with the subsequent cooling in the expansion. The low temperatures in the jet not only simplify the spectral complexity, but also substantially enhance the sensitivity, because the population is concentrated in the lowest energy states only.

It is important that both jaws have negative polarity with respect to the grounded plate. As has been pointed out in Ref. 23 this sensitivity to the sign of the bias is caused by the large difference in mobility between the negative and positive charge carriers in the plasma. A large positive voltage

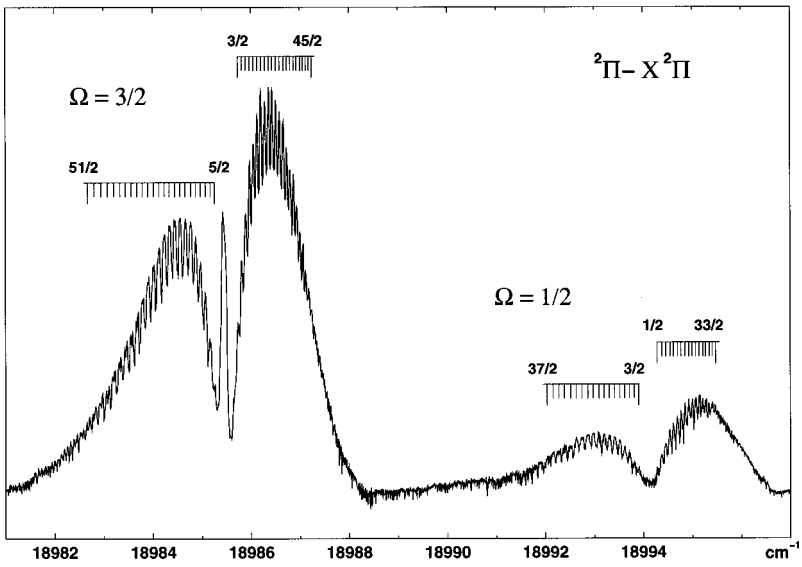

FIG. 4. The rotationally resolved spin-orbit components of the origin band of the $^2\Pi \leftarrow X^2\Pi$ electronic transition of C_6H measured in a supersonic slit jet plasma, employing cavity ring down detection. The assignment is given in the figure. The rotational temperature amounts to ≈15 K.

across the jaws results in a less stable discharge with much lower discharge currents and lower production rates accordingly. However, for the production of positively charged ions this configuration may be less favorable. Therefore, in the case of cations a grid is mounted about 20 mm downstream of the nozzle orifice and it carries a negative voltage in order to compensate for the effect. The value of the discharge current is determined by the applied voltage and the ballast resistors. Slightly better signal-to-noise ratios are obtained by using smaller resistors, but this also favors soot formation in the nozzle.

C. Time sequence

The whole experiment runs at 30 Hz. A master trigger is sent to a delay generator from which the excimer laser, gas valve, and discharge pulse are triggered independently. The timing of the experiment is shown in Fig. 3 (upper trace). A 1:100 voltage divider is connected to the slit plates to monitor the discharge. The width of the discharge pulse is chosen to last 150 μs, which is slightly longer than the typical time in which the light pulse is confined to the optical cavity. The gas pulse is considerably longer and can be monitored by increasing the discharge time. In Fig. 3 (lower trace) the gas pulse through the slit is shown for an opening time of the pulsed valve on top of the body of 600 μs (11 bar backing pressure). The actual expansion through the slit lasts about 1100 μs. On the time scale of the ring down experiment the expansion (i.e., discharge current) can be considered to be stationary. This diagram also yields information on the actual (I,V) characteristics of the discharge. The voltage drop over the ballast resistor directly yields the discharge current for one jaw (typically 60–120 mA). The remaining voltage is the actual potential difference between the jaws and the grounded metal plate.

III. RESULTS AND DISCUSSION

In the next paragraphs results on C_6H, $C_6H_2^+$ and C_2^- are presented. The reason for focusing on carbon radicals is twofold. First, long carbon chain radicals are important from a chemical point of view. They play a role as reactive intermediates in fullerene formation and are among the attractive candidates of diffuse interstellar band carriers.[49] A wealth of information is available from absorption spectra of mass-selected species in solid neon matrixes.[50] Ground state rotation and vibration spectra have been obtained in the gas phase, using direct absorption spectroscopic techniques.[51–53] The gas phase electronic spectra of several carbon chain anions have been observed, using resonant enhanced multiphoton electron detachment (see, e.g., Refs. 54–56) and recently, electronic spectra of neutral carbon chains were found as well.[24,26,36] Second, since carbon tends to form conducting layers and as such might short-circuit a discharge, a carbon plasma is a rather severe test to check the stable performance of the source.

A. C_6H

Figure 4 shows the rotationally resolved spin-orbit components of the $^2\Pi \leftarrow X^2\Pi$ electronic origin band transition of C_6H around 18 989 cm^{-1}. The search for this band was initially guided by results obtained for mass selected C_6H in a 5 K solid neon matrix around 18 844 cm^{-1}.[57] The observed 145 cm^{-1} shift is consistent with values found for isoelectronic species and carbon chains of comparable length.[50] As for all $C_{2n}H$ species with $n>2$, C_6H has an inverted $^2\Pi$ ground state. For $^2\Pi \leftarrow X^2\Pi$ transitions one expects to observe both the $\Omega=\frac{3}{2}$ and $\frac{1}{2}$ components in the electronic spectrum, separated by the difference of the spin-orbit constants $|A'-A''|$ and consisting of P, Q, and R branches.

The relative intensity of both spin-orbit components is strongly influenced by the low rotational temperatures in the jet and the size of the spin-orbit splitting in the ground state $(A''=-15.11$ cm$^{-1})$.[58] Both the rotational profile and the relative intensity of the spin-orbit components yield a rotational temperature of (15 ± 5) K. This low temperature allows in contrast with previous CRDS measurements in a hollow cathode cell,[36] a direct assignment of the $^2\Pi_{1/2} \leftarrow X^2\Pi_{1/2}$ and $^2\Pi_{3/2} \leftarrow X^2\Pi_{3/2}$ electronic bands, as in the jet the $\Omega=\frac{3}{2}$ component will be substantially more populated than the $\Omega=\frac{1}{2}$ component. For this reason the band to lower energy has to

be assigned to the $^2\Pi_{3/2}\leftarrow X^2\Pi_{3/2}$ system. This implies that the spin-orbit splitting in the excited state is larger than in the ground state, as has been explained in Ref. 24. In addition, it is expected that the $^2\Pi_{3/2}\leftarrow X^2\Pi_{3/2}$ band will have a more pronounced Q-branch pattern than the $^2\Pi_{1/2}\leftarrow X^2\Pi_{1/2}$ band, since the intensity of the Q branch is proportional to Ω^2, which can be seen in Fig. 4 as well. By inserting an etalon in the dye laser cavity, a bandwidth of 0.035 cm^{-1} can be achieved which is of the same order of magnitude as the rotational constant of C_6H. Consequently, since slit nozzle expansions are generally Doppler free, rotationally resolved spectra have been measured. Typically, linewidths (full width at half maximum) of the order of 0.037 cm^{-1} have been obtained. In Fig. 4 the rotational assignment for both spin-orbit components is given as well. For the strong band a gap of ≈10 B and for the weaker band a gap of ≈6 B is found which agrees with the assignment to the $\Omega=\frac{3}{2}$ and $\frac{1}{2}$ component, respectively. Accurate constants for the excited state have been calculated, using ground state constants obtained in previous microwave work.[58] These results, together with those on C_6D, will be presented elsewhere.[59]

B. Chemistry in the jet

In a similar way as described for C_6H and C_6D, spectra have been obtained for C_8H/C_8D and $C_{10}H/C_{10}D$.[26] In Ref. 23 it was discussed that the short residence time of the radical precursors in the discharge zone does not allow secondary radical–radical reactions. Consequently, the long carbon chains are expected to be formed by multiple collisions in the expanding plasma. The present technique is ideally suited to study the C_nH density as a function of the distance to the nozzle orifice. The product $(I\cdot r)$ of the integrated C_8H signal (I) and the distance to the nozzle orifice (r) as a function of r is shown in Fig. 5. Whereas normally an r^{-1} density decrease is expected as a consequence of the two-dimensional character of the expansion,[10] i.e., the product of I and r should yield a constant value—this is different for C_8H. The C_8H is formed in the first millimeters after the orifice in the collision regime of the expansion and reaches its equilibrium point for a backing pressure of 10 bar about 8 mm downstream. After 8 mm the $I(C_8H)$ signal starts to show r^{-1} behavior.

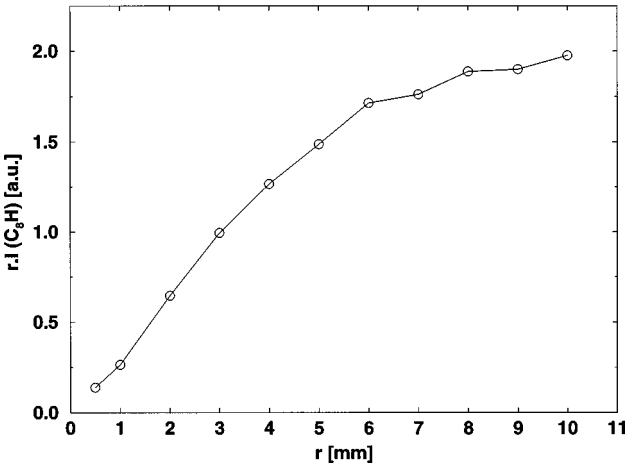

FIG. 5. The product $(r\cdot I)$ of the distance to the nozzle orifice (r) and the total integrated C_8H signal (I), as function of r. For slit nozzles this value is constant, due to the two-dimensional character of the expansion, unless a molecule is being formed in the expansion, which is clearly the case for C_8H.

C. $C_6H_2^+$

The triacetylene cation is isoelectronic with C_6H and consequently the electronic spectra of both systems should be similar. In the past, several gas phase studies have been performed on the origin band of the $^2\Pi\leftarrow X^2\Pi$ electronic transition of $C_6H_2^+$, mainly in low resolution emission experiments.[60,61] In a recent study in a hollow cathode White cell geometry ($T_{rot}\approx 170$ K)[62] also rotationally resolved optical absorption spectra of both spin-orbit components of $C_6H_2^+$ and its isotopic derivatives $C_6D_2^+$ and HC_6D+ have been obtained. In the latter experiment the band origin of the

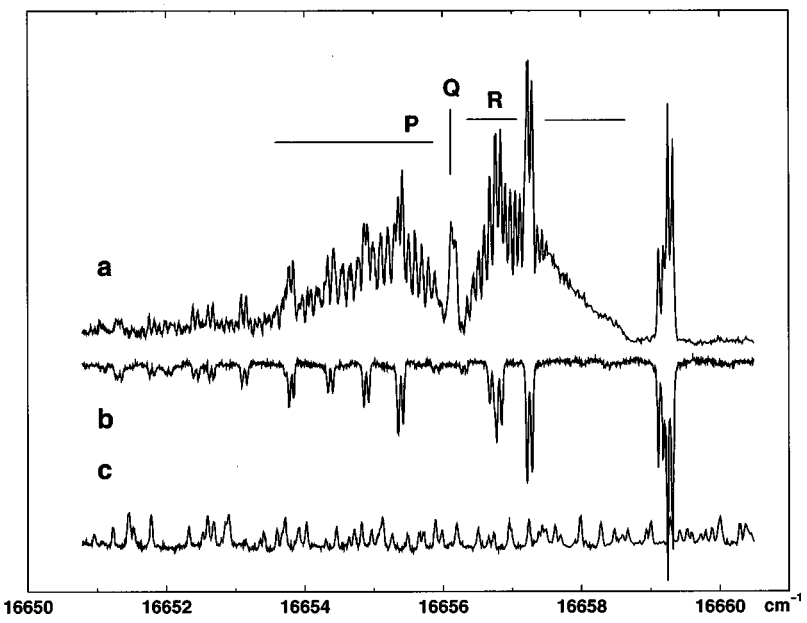

FIG. 6. The rotationally resolved $\Omega=\frac{3}{2}$ origin band of the $^2\Pi\leftarrow X^2\Pi$ electronic transition of the triacetylene cation $C_6H_2^+$. (a) The spectrum in a C_2H_2/He plasma. The spectrum is clearly covered with additional lines. These originate from a pure carbon species (C_2 here), as can be concluded from (b), showing the same frequency range in a C_2D_2/He plasma. (c) The iodine spectrum that is recorded simultaneously for linearization and absolute calibration.

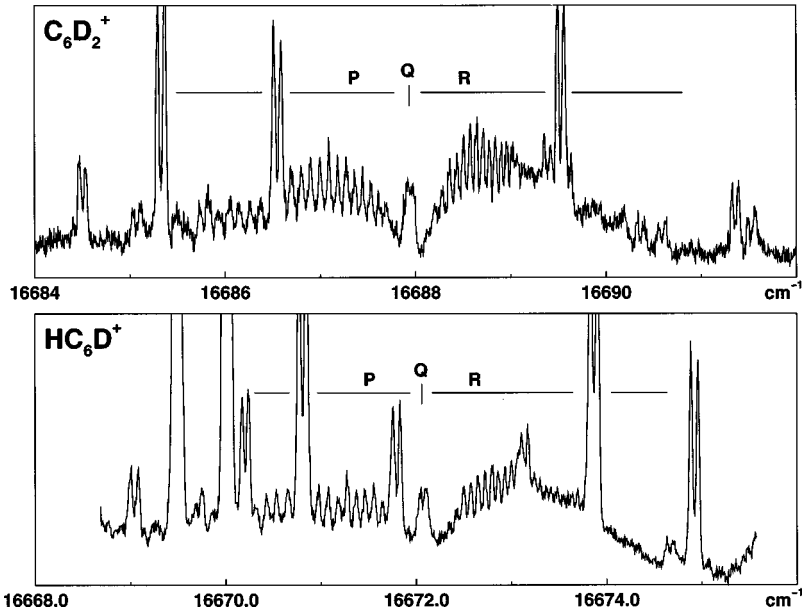

FIG. 7. The rotationally resolved $\Omega=\frac{3}{2}$ origin band of the $^2\Pi\leftarrow X^2\Pi$ electronic transition of $C_6D_2^+$ (upper trace) and HC_6D^+ (lower trace), using a mixture of 0.25% C_2D_2 and C_2H_2/C_2D_2 (1:3) in He, respectively.

$\Omega=\frac{3}{2}$ component of $C_6H_2^+$ is found at 16 656.2 cm^{-1}, about 3 cm^{-1} to higher energy than the $\Omega=\frac{1}{2}$ component, indicating that $|A'|<|A''|$.

In Fig. 6(a) the rotationally resolved origin band of the $^2\Pi\leftarrow X^2\Pi$ electronic transition of $C_6H_2^+$ is shown, recorded in the present jet experiment. The best signal-to-noise ratios were obtained for voltages around -550 V. Only one subband can be observed now, because the spin-orbit splitting in the ground state with $-31.40(28)$ cm^{-1} (Ref. 62) is rather large and consequently the population of the $\Omega=\frac{1}{2}$ component will be only moderate at the low temperatures in the jet. Furthermore, it is expected that the $\Omega=\frac{1}{2}$ component will be hidden under the P branch of the $\Omega=\frac{3}{2}$ component since the value of $|A'-A''|\approx 3$ cm^{-1} is too small to separate both spin-orbit components completely, as is the case for C_6H. The $C_6H_2^+$ spectrum is partially covered with lines that originate from C_2. In Fig. 6(b) the same frequency range is shown, but for a C_2D_2/He plasma: only the pure carbon signals remain. The resulting $0_0^0\,^2\Pi\leftarrow X^2\Pi$ spectrum for $C_6D_2^+$ ($\Omega=\frac{3}{2}$ component) is blue shifted by 32 cm^{-1} (Fig. 7, upper trace). A 1:3 C_2H_2/C_2D_2 (0.25%) in He mixture yields the corresponding spectrum of HC_6D^+ (Fig. 7, lower trace). These figures also show that the appropriate choice of isotopic species can make up for the disadvantage of having no mass selectivity.

The spectra are reproduced with the rotational constants derived in Ref. 62 and assuming a rotational temperature of (10 ± 3) K. The low temperature can be achieved in spite of an additional grid that is mounted about 2 cm downstream of the nozzle orifice. This grid is put on a negative potential, which improved signal-to-noise ratios by extracting the positive ions out of the field of the nozzle jaws. However, it also causes minor disturbances in the dynamic flow of the gas expansion, which might effectively decrease the adiabatic cooling. The geometry without grid should also allow the detection of anions.

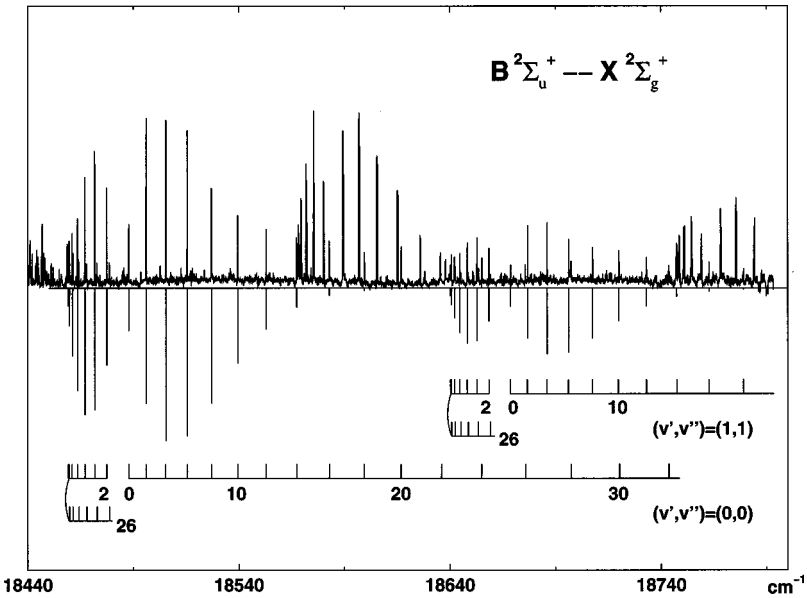

FIG. 8. The P and R branches of the $(v',v'')=(0,0)$ and (1,1) vibrational transitions in the $B^2\Sigma_u^+\leftarrow X^2\Sigma_g^+$ electronic spectrum of C_2^-, measured with CRDS. The simulation uses the constants given in Ref. 69. The unassigned band around 18 590 cm^{-1} belongs to C_2.

D. C_2^-

Rovibrationally resolved spectra of negative ions have been obtained mainly by velocity modulation ($v''=0$) and photodetachment ($v''\geqslant 0$) (Refs. 6 and 63). Here it is demonstrated that the current setup can be used as a sensitive probe to study vibrationally excited negative ions as well and it is expected that this technique may serve as a more general tool for the study of electronic transitions of anions. The *electronic* spectroscopy of anions is normally limited by molecule specific properties, such as optically accessible excited states below the detachment threshold, which determines whether anion zero electron kinetic energy[64] or autodetachment spectroscopy[63,65] are applicable. These problems do not exist with a method based on direct absorption. In Fig. 8 rotationally resolved vibration bands of the $B^2\Sigma_u^+ \leftarrow X^2\Sigma_g^+$ electronic transition of C_2^- are shown, measured with the current setup. This electronic transition was first observed in a flash absorption experiment in CH_4 (Ref. 66) and its assignment was confirmed later by photodetachment techniques.[67] The lifetimes of rotational levels of the B state ($v'=0$ and $v'=1$) and the oscillator strength f_{00} were determined as well.[68] Consequently, the anion is well characterized, allowing a straightforward assignment.

In Fig. 8 the P and R branches of the $(v',v'')=(0,0)$ and (1,1) bands are shown. The signal-to-noise ratio for the strongest signals amounts to ≈ 50 and is obtained for measurements close to the slit nozzle orifice (≈ 3 mm). This explains that the spectrum can only be reproduced with a rather high rotational temperature (150 K). The resulting simulation (see Fig. 8) does not exactly match the rotational contour, which is mainly due to the different rotational temperature regimes for low and high J levels.[31] This effect is even enhanced because C_2^- has a relatively large rotational constant. The spectrum also shows that the vibrational degrees of freedom are not cooled as effectively as the rotational ones.

C_2^- is special as anion in the way that it possesses a bound valence state below the continuum. This special characteristic results from the high electron affinity of C_2 and the low electronic excited states of C_2^-. For negative ions in general, the number of bound states is rather limited. But even in the case where an anion only has a repulsive excited state, CRDS offers in principal a possible probe, because it is intrinsically based upon the direct absorption of light and consequently there are no restrictions regarding the nature of the excited state. Furthermore it directly allows the determination of absolute densities, applying Beer Lambert's law. The concentration $[C_2^-]$ is calculated from the oscillator strength $f_{00}=0.044$,[68] the exact absorption pathlength and the total integrated absorption coefficient, which yields an absolute density of $\approx 4\times 10^8$ molecules/cm^3. With the current signal-to-noise ratios, this gives a lower detection limit of approximately 10^7 C_2^--ions/cm^3.

ACKNOWLEDGMENTS

The authors thank Dr. Markus Kotterer for help during the initial stage of the experiments. This work is part of Project No. 20-29104.96 of the Swiss National Science Foundation.

[1] T. Oka, in *Frontiers of Laser Spectroscopy of Gases*, edited by A. C. P. Alves, J. M. Brown, and J. M. Hollas (Kluwer Academic, Dordrecht, 1988), pp. 353–378.
[2] R. C. Woods, in *Ion and Cluster Ion Spectroscopy and Structure*, edited by J. P. Maier (Elsevier Science, New York, 1989), pp. 27–58.
[3] J. V. Coe and R. J. Saykally, in *Ion and Cluster Ion Spectroscopy and Structure*, edited by J. P. Maier (Elsevier Science, Amsterdam, 1989), pp. 106–131.
[4] F. C. van den Heuvel and A. Dymanus, Chem. Phys. Lett. **92**, 219 (1982).
[5] F. C. de Lucia, E. Herbst, G. Plummer, and G. Blake, J. Chem. Phys. **78**, 2312 (1983).
[6] C. S. Gudeman, M. H. Begemann, J. Pfaff, and R. J. Saykally, Phys. Rev. Lett. **50**, 727 (1983).
[7] A. T. Droege and P. C. Engelking, Chem. Phys. Lett. **96**, 316 (1983).
[8] P. C. Engelking, Rev. Sci. Instrum. **57**, 2274 (1986).
[9] P. C. Engelking, Chem. Rev. **91**, 399 (1991).
[10] M. Sulkes, C. Jouvet, and S. A. Rice, Chem. Phys. Lett. **87**, 515 (1982).
[11] K. L. Busarow, G. A. Blake, K. B. Laughlin, R. C. Cohen, Y. T. Lee, and R. J. Saykally, Chem. Phys. Lett. **141**, 289 (1987).
[12] D. J. Nesbitt, Chem. Rev. **88**, 843 (1988).
[13] A. van Orden and R. J. Saykally, Chem. Rev. **98**, 2313 (1988).
[14] T. F. Giesen, A. van Orden, H. J. Hwang, R. S. Fellers, R. A. Provençal, and R. J. Saykally, Science **265**, 756 (1994).
[15] R. F. Curl, K. K. Murray, M. Petri, M. L. Richnow, and F. K. Tittel, Chem. Phys. Lett. **161**, 98 (1989).
[16] Y. Sumiyoshi, T. Imajo, K. Tanaka, and T. Tanaka, Chem. Phys. Lett. **231**, 569 (1994).
[17] K. R. Comer and S. C. Foster, Chem. Phys. Lett. **202**, 216 (1993).
[18] G. Hilpert, H. Linnartz, M. Havenith, J. J. ter Meulen, and W. L. Meerts, Chem. Phys. Lett. **219**, 384 (1994).
[19] M. Fukushima, M. C. Chan, Y. Xu, A. Taleb-Bendiab, and T. Amano, Chem. Phys. Lett. **230**, 561 (1994).
[20] K. Harada and T. Tanaka, Chem. Phys. Lett. **227**, 651 (1994).
[21] Y. Xu, M. Fukushima, T. Amano, and A. R. W. McKellar, Chem. Phys. Lett. **242**, 126 (1995).
[22] D. T. Anderson, S. Davis, T. S. Zwier, and D. J. Nesbitt, Chem. Phys. Lett. **258**, 207 (1996).
[23] S. Davis, D. T. Anderson, G. Duxbury, and D. J. Nesbitt, J. Chem. Phys. **107**, 5661 (1997).
[24] D. A. Kirkwood, H. Linnartz, M. Grutter, O. Dopfer, T. Motylewski, M. Pachkov, M. Tulej, M. Wyss, and J. P. Maier, Faraday Discuss. **109**, 109 (1998).
[25] H. Linnartz, T. Motylewski, F. Maiwald, D. A. Roth, F. Lewen, I. Pak, and G. Winnewisser, Chem. Phys. Lett. **292**, 188 (1998).
[26] H. Linnartz, T. Motylewski, and J. P. Maier, J. Chem. Phys. **109**, 3819 (1998).
[27] T. Ruchti, A. Rohrbacher, T. Speck, J. P. Connelly, E. J. Bieske, and J. P. Maier, Chem. Phys. **209**, 169 (1996).
[28] T. Speck, H. Linnartz, and J. P. Maier, J. Chem. Phys. **107**, 8706 (1997).
[29] H. Linnartz, T. Speck, and J. P. Maier, Chem. Phys. Lett. **288**, 504 (1998).
[30] T. Ruchti, T. Speck, J. P. Connelly, E. J. Bieske, H. Linnartz, and J. P. Maier, J. Chem. Phys. **105**, 2591 (1996).
[31] T. Speck, T. Ruchti, H. Linnartz, and J. P. Maier, J. Mol. Spectrosc. **185**, 425 (1997).
[32] A. O'Keefe and D. A. G. Deacon, Rev. Sci. Instrum. **59**, 2544 (1988).
[33] J. J. Scherer, D. Voelkel, and D. J. Rakestraw, Appl. Phys. B: Lasers Opt. **64**, 699 (1997).
[34] G. Berden, R. Engeln, P. C. M. Christianen, J. C. Maan, and G. Meijer, Phys. Rev. A **58**, 3114 (1998).
[35] M. Kotterer, J. Conceiçao, and J. P. Maier, Chem. Phys. Lett. **259**, 233 (1996).
[36] M. Kotterer and J. P. Maier, Chem. Phys. Lett. **266**, 342 (1997).
[37] R. A. Provençal, J. B. Paul, E. Michael, and R. J. Saykally, Photonics Spectra **6**, 159 (1998).
[38] A. O'Keefe, J. J. Scherer, A. L. Cooksy, R. Sheeks, J. Heath, and R. J. Saykally, Chem. Phys. Lett. **172**, 214 (1990).
[39] D. Romanini, A. A. Kachanov, N. Sadeghi, and F. Stoeckel, Chem. Phys. Lett. **264**, 316 (1997).
[40] J. B. Paul, C. P. Collier, R. J. Saykally, J. J. Scherer, and A. O'Keefe, J. Phys. Chem. A **1091**, 5211 (1997).
[41] A. A. Ruth, T. Fernholz, R. P. Brint, and M. W. D. Mansfield, Chem. Phys. Lett. **287**, 403 (1998).
[42] D. Romanini, A. A. Kachanov, and F. Stoeckel, Chem. Phys. Lett. **270**, 546 (1997).

[43] Y. He, M. Hippler, and M. Quack, Chem. Phys. Lett. **289**, 527 (1998).
[44] R. Engeln and G. Meijer, Rev. Sci. Instrum. **67**, 2708 (1996).
[45] R. Engeln, E. van den Berg, G. Meijer, L. Lin, G. M. H. Knippels, and A. F. G. van der Meer, Chem. Phys. Lett. **269**, 293 (1997).
[46] C. J. Chapo, J. B. Paul, K. Roth, and R. J. Saykally, 53rd International Symposium on High Resolution Molecular Spectroscopy, Columbus, OH, 15–19 June, contribution TE09.
[47] J. J. Scherer, J. B. Paul, A. O'Keefe, and R. J. Saykally, Chem. Rev. **97**, 25 (1997).
[48] M. D. Wheeler, S. M. Newman, A. J. Orr-Ewing, and N. R. Ashfold, J. Chem. Soc., Faraday Trans. **94**, 337 (1998).
[49] A. E. Douglas, Nature (London) **269**, 130 (1977).
[50] J. P. Maier, Chem. Soc. Rev. **26**, 21 (1997).
[51] J. R. Heath and R. J. Saykally, *On Clusters and Clustering, from Atoms to Fractals*, edited by P. J. Reynolds (Elsevier Science, New York, 1993), pp. 7–21.
[52] M. C. McCarthy, M. J. Travers, A. Kovács, C. A. Gottlieb, and P. Thaddeus, Astrophys. J., Suppl. Ser. **113**, 105 (1997).
[53] P. Thaddeus, M. C. McCarthy, M. J. Travers, C. A. Gottlieb, and W. Chen, Faraday Discuss. **109**, 121 (1998).
[54] M. Ohara, H. Shiromaru, and Y. Achiba, J. Chem. Phys. **106**, 9992 (1997).
[55] Y. Zhao, E. de Beer, C. Xu, T. Taylor, and D. M. Neumark, J. Chem. Phys. **105**, 4905 (1996).
[56] M. Tulej, D. A. Kirkwood, G. Maccaferri, O. Dopfer, and J. P. Maier, Chem. Phys. **128**, 239 (1998).
[57] P. Freivogel, J. Fulara, M. Jakobi, D. Forney, and J. P. Maier, J. Chem. Phys. **103**, 54 (1995).
[58] J. C. Pearson, C. A. Gottlieb, D. R. Woodward, and P. Thaddeus, Astron. Astrophys. **189**, L13 (1988).
[59] H. Linnartz, T. Motylewski, O. Vaizert, J. P. Maier, A. J. Apponi, M. C. McCarthy, C. A. Gottlieb, and P. Thaddeus, J. Chem. Phys. (in preparation).
[60] M. Allan, E. Kloster-Jensen, and J. P. Maier, J. Chem. Phys. **7**, 11 (1976).
[61] D. Klapstein, R. Kuhn, J. P. Maier, M. Ochsner, and W. Zambach, J. Phys. Chem. **88**, 5176 (1984).
[62] W. E. Sinclair, D. Pfluger, H. Linnartz, and J. P. Maier, J. Chem. Phys. (in press).
[63] E. de Beer, Y. Zhao, I. Yourshaw, and D. M. Neumark, Chem. Phys. Lett. **244**, 400 (1995).
[64] C. C. Arnold and D. M. Neumark, J. Chem. Phys. **99**, 3353 (1993); Can. J. Phys. **72**, 1322 (1994).
[65] K. R. Lykke, T. Andersen, and D. M. Neumark, J. Chem. Phys. **83**, 4364 (1985).
[66] G. Herzberg and A. Lagerqvist, Can. J. Phys. **46**, 2365 (1968).
[67] W. C. Lineberger and T. A. Patterson, Chem. Phys. Lett. **13**, 40 (1972).
[68] S. Leutwyler, J. P. Maier, and L. Misev, Chem. Phys. Lett. **91**, 206 (1982).
[69] P. L. Jones, R. D. Mead, B. E. Kohler, S. D. Rosner, and W. C. Lineberger, J. Chem. Phys. **73**, 4419 (1980).